

ACT-05/96
DOE/ER/40717-26
CTP-TAMU-13/96
hep-ph/9605419

Enhanced Supersymmetric Corrections to Top-Quark Production at the Tevatron

Jaewan Kim¹, Jorge L. Lopez², D.V. Nanopoulos^{1,3}, and R. Rangarajan¹

¹Astroparticle Physics Group, Houston Advanced Research Center (HARC)
The Mitchell Campus, The Woodlands, TX 77381, USA

²Department of Physics, Bonner Nuclear Lab, Rice University
6100 Main Street, Houston, TX 77005, USA

³Center for Theoretical Physics, Department of Physics, Texas A&M University
College Station, TX 77843-4242, USA

Abstract

We calculate the one-loop supersymmetric electroweak and QCD corrections to the top-quark pair-production cross section at the Tevatron, including the important effects of non-degenerate top-squarks and left-right top-squark mixing. The largest electroweak effects yield a negative shift in the cross section and are enhanced right below the threshold for top-quark decay into top-squark and higgsino-like neutralino, and can be as large as -35% . The largest QCD effects are positive and are enhanced for light top-squark masses, and can be as large as 20% . Such shifts greatly exceed the present theoretical uncertainty in the Standard Model prediction, and therefore may be experimentally observable. We also explore the one-loop shifts in scenarios containing light top-squarks and higgsino-like neutralinos, that have been recently proposed to explain various apparent experimental anomalies.

ACT-05/96
DOE/ER/40717-26
CTP-TAMU-13/96
May 1996

1 Introduction

The existence of the top quark has now been firmly established by the CDF and D0 Collaborations at Fermilab [1]. The analysis of over 100 pb^{-1} of data by each experiment has allowed a determination of the top-quark mass and pair-production cross section [2]

$$m_t^{\text{CDF}} = 176 \pm 9 \text{ GeV}, \quad \sigma_{t\bar{t}}^{\text{CDF}} = 7.6_{-1.5}^{+1.9} \text{ pb}; \quad (1)$$

$$m_t^{\text{D0}} = 170 \pm 18 \text{ GeV}, \quad \sigma_{t\bar{t}}^{\text{D0}} = 5.2 \pm 1.8 \text{ pb}; \quad (2)$$

to better than $\sim 5\%$ and $\sim 20\%$ respectively. The experimental error flags are expected to be further reduced when the data set is fully analyzed. A significant increase in sensitivity will become available once the Main Injector upgrade becomes operational in 1999, with an expected reduction in the top-quark mass uncertainty down to 3.5 (2.0) GeV and in the production cross section down to 11% (6%) with an integrated luminosity of $\mathcal{L} = 1 (10) \text{ fb}^{-1}$ [3]. On the other hand, the theoretical prediction for the cross section in the Standard Model has become rather precise [4, 5, 6], and is presently known to better than 10% for fixed values of m_t , *e.g.* [5]

$$\sigma_{t\bar{t}}^{\text{theory}} [170] = 6.48_{-0.48}^{+0.09} \text{ pb}, \quad \sigma_{t\bar{t}}^{\text{theory}} [175] = 5.52_{-0.42}^{+0.07} \text{ pb}. \quad (3)$$

The agreement between theoretical expectations and experimental observations is not tight enough to preclude moderate shifts ($\sim 2 \text{ pb}$) to the production cross section from new physics phenomena. However, greater than 50% shifts in the Standard Model prediction, *i.e.*, exceeding twice the present experimental uncertainty, appear disfavored. It is then opportune to investigate how large a shift may scenarios for new physics yield, most interestingly in the case of low-energy supersymmetry.

In this paper we consider the one-loop corrections to the pair-production cross section for top quarks at the Tevatron, including both electroweak (loops of charginos and bottom-squarks or neutralinos and top-squarks) and QCD (loops of gluinos and squarks) contributions. Our calculation extends and corrects those in the literature [7, 8], identifies the largest contributions and determines under what conditions they may be enhanced, and treats all important and realistic effects (such as top-squark mass non-degeneracy and mixing) in a unified way. We also consider specific scenarios with especially light supersymmetric particles that have been proposed in connection with the R_b observable [9], an as-yet unexcluded light higgsino window [10], and a possible supersymmetric explanation [11, 12] for the $ee\gamma\gamma$ event observed by CDF [13]. We stress that light supersymmetric particles that affect the top-quark cross section are also likely to affect its decay width via new supersymmetric channels, and the resulting decrease in $B(t \rightarrow bW)$ may affect the yield of $bWbW$ events in a much more significant way than a shift in the underlying production cross section.

This paper is organized as follows. In Sec. 2 we present compact expressions for the results of our analytical calculations for the one-loop supersymmetric electroweak and QCD corrections, and contrast them with existing calculations. In Sec. 3 we present a qualitative and quantitative study of the expected corrections, and identify

a ‘best case scenario’ that entails the largest possible effects. These effects may easily exceed the theoretical uncertainty in the Standard Model prediction for the top-quark cross section, and thus may be disentangled at future Tevatron runs. In Sec. 4 we adapt our general results to study specific models that have been proposed in the literature and that contain especially light supersymmetric particles. Sec. 5 summarizes our conclusions.

2 Analytical results

Top-quark pair-production at a hadron collider proceeds at tree-level via two underlying s -channel parton processes: $q\bar{q}$ annihilation and gluon fusion. At the Tevatron the first process dominates (90%), and therefore we neglect the latter in what follows. One-loop corrections to $q\bar{q} \rightarrow g \rightarrow t\bar{t}$ in the context of low-energy supersymmetry fall into two categories: electroweak-like [7] and QCD-like [8]. The electroweak-like corrections modify the outgoing part of the Feynman diagram via new contributions to the $g t\bar{t}$ vertex and to the normalization of the top-quark wavefunction, that involve loops of top-squarks and neutralinos or bottom-squarks and charginos. The QCD-like corrections modify both the incoming and outgoing portions of the diagram in an analogous fashion, but this time involving loops of gluinos and first-generation-squarks or gluinos and top-squarks. (In the case of the QCD-like corrections, there are also (smaller) box diagram contributions involving gluinos and squarks.)

The tree-level $q\bar{q} \rightarrow t\bar{t}$ parton cross section is given by

$$\hat{\sigma} = \frac{8\pi\alpha_s^2}{9\hat{s}^2} \beta_t \frac{1}{3}(\hat{s} + 2m_t^2) \quad (4)$$

where $\beta_t = \sqrt{1 - 4m_t^2/\hat{s}}$, and $\sqrt{\hat{s}}$ is the usual parton-level center-of-mass energy. The supersymmetric electroweak-like one-loop corrections are enhanced by a large top-quark Yukawa coupling and thus involve loops of top-squarks and neutralinos or bottom-squarks and charginos, as the decomposition of the top-quark Yukawa coupling shows

$$\lambda_t Q_3 \widetilde{H}_2 \tilde{t}_R \rightarrow \lambda_t b_L \widetilde{H}^\pm \tilde{t}_R, \quad \lambda_t t_L \widetilde{H}_2^0 \tilde{t}_R, \quad (5)$$

which picks out $\tilde{t} \rightarrow \tilde{t}_R$, $\chi^\pm \rightarrow \widetilde{H}^\pm$, $\chi^0 \rightarrow \widetilde{H}_2^0$, *i.e.*, the higgsino components of the chargino and neutralino. These one-loop contributions are given by

$$\Delta\hat{\sigma}^{\text{EW}} = \frac{8\pi\alpha_s^2}{9\hat{s}^2} \beta_t \left(\frac{\lambda_t}{4\pi} \right)^2 \left[\frac{2}{3}(\hat{s} + 2m_t^2)(F_1^n + F_1^c) + 2(F_5^n + F_5^c)m_t\hat{s} \right], \quad (6)$$

where $\lambda_t = m_t/(\frac{v_0}{\sqrt{2}} \sin \beta)$ is the top-quark Yukawa coupling, with $v_0 \approx 246$ GeV the usual Standard Model Higgs vacuum expectation value, and $\tan \beta = v_2/v_1$ the ratio of the two Higgs vacuum expectation values that arise in the MSSM. Also, $F_{1,5}^{n,c}$ are form factors that encode the loop functions and depend on the various mass parameters.

The top-squark–neutralino form factors are given by:

$$\begin{aligned}
F_1^n &= \sum_{j=1}^4 \left\{ N_{j4} N_{j4}^* \sum_{J=1}^2 \left[c_{24} + m_t^2 (c_{11} + c_{21}) + \frac{1}{2} B_1 + m_t^2 B_1' \right]^{(\chi_j^0, \tilde{t}_J, \tilde{t}_J)} \right. \\
&\quad \left. - \text{Re} (N_{j4} N_{j4}) \sum_{J=1}^2 (-1)^{J+1} \sin(2\theta_t) m_t m_{\chi_j^0} (c_0 + c_{11} + B_0')^{(\chi_j^0, \tilde{t}_J, \tilde{t}_J)} \right\}; \quad (7) \\
F_5^n &= \sum_{j=1}^4 \left\{ N_{j4} N_{j4}^* \sum_{J=1}^2 \left[-\frac{1}{2} m_t (c_{11} + c_{21}) \right]^{(\chi_j^0, \tilde{t}_J, \tilde{t}_J)} \right. \\
&\quad \left. + \text{Re} (N_{j4} N_{j4}) \sum_{J=1}^2 (-1)^{J+1} \frac{1}{2} \sin(2\theta_t) m_{\chi_j^0} (c_0 + c_{11})^{(\chi_j^0, \tilde{t}_J, \tilde{t}_J)} \right\}. \quad (8)
\end{aligned}$$

Here N_{j4} represents the higgsino admixture of χ_j^0 (\widetilde{H}_2^0 in the notation of Eq. (5) and Ref. [14]), and the $J = 1, 2$ sum runs over the two top-squark mass eigenstates ($m_{\tilde{t}_{1,2}}$), which are obtained from the $\tilde{t}_{L,R}$ gauge eigenstates via: $\tilde{t}_1 = \cos \theta_t \tilde{t}_L + \sin \theta_t \tilde{t}_R$ and $\tilde{t}_2 = -\sin \theta_t \tilde{t}_L + \cos \theta_t \tilde{t}_R$. The various B and c functions in the above expressions are the well documented Passarino-Veltman functions [15] (adapted to our metric where $p_i^2 = m_i^2$); the B functions depend on $(m_t, m_{\chi_j^0}, m_{\tilde{t}_J})$ whereas the c functions depend on $(-p_3, p_3 + p_4, m_{\chi_j^0}, m_{\tilde{t}_J}, m_{\tilde{t}_J})$ [as reminded by the superscripts in Eqs. (7,8)], where p_3 and p_4 are the momenta of the outgoing top-quark and anti-top-quark respectively. The bottom-squark–chargino form factors are in turn given by

$$\begin{aligned}
F_1^c &= \sum_{j=1}^2 V_{j2} V_{j2}^* \sum_{J=1}^2 \left(\frac{\cos^2 \theta_b^{(J=1)}}{\sin^2 \theta_b^{(J=2)}} \right) \left[c_{24} + m_t^2 (c_{11} + c_{21}) + \frac{1}{2} B_1 + m_t^2 B_1' \right]^{(\chi_j^\pm, \tilde{b}_J, \tilde{b}_J)} \quad (9) \\
F_5^c &= \sum_{j=1}^2 V_{j2} V_{j2}^* \sum_{J=1}^2 \left(\frac{\cos^2 \theta_b^{(J=1)}}{\sin^2 \theta_b^{(J=2)}} \right) \left[-\frac{1}{2} m_t (c_{11} + c_{21}) \right]^{(\chi_j^\pm, \tilde{b}_J, \tilde{b}_J)}, \quad (10)
\end{aligned}$$

where V_{j2} represents the higgsino admixture of χ_j^\pm , and for completeness we have allowed a non-vanishing bottom-squark mixing angle such that $\tilde{b}_1 = \cos \theta_b \tilde{b}_L + \sin \theta_b \tilde{b}_R$ and $\tilde{b}_2 = -\sin \theta_b \tilde{b}_L + \cos \theta_b \tilde{b}_R$. The $J = 1, 2$ sum runs over the two bottom-squark mass eigenstates ($m_{\tilde{b}_{1,2}}$). Note that if $\theta_b = 0$, only the left-handed bottom-squark is involved in the loops. In this case the B functions depend on $(m_t, m_{\chi_j^\pm}, m_{\tilde{b}_J})$ whereas the c functions depend on $(-p_3, p_3 + p_4, m_{\chi_j^\pm}, m_{\tilde{b}_J}, m_{\tilde{b}_J})$. Since the Passarino-Veltman functions can be notoriously difficult to evaluate numerically for certain values of the parameters, we have employed different methods (all of which agree), in particular using the software package **ff** [16]. Our results for the case of no top- or bottom-squark mixing ($\theta_t = \theta_b = 0$) disagree with those originally published in Ref. [7]. However, these authors have since revised their calculation and their corrected expressions [17] are now in agreement with our results above. Our results for the realistic case of squark mixing ($\theta_t, \theta_b \neq 0$) are new.¹

¹While the present paper was being written up Ref. [18] appeared, which contains a calculation of the $\theta_t \neq 0$ case, that agrees with our result above in the case of real N_{j4} values.

In Eqs. (6,7,8,9,10) we have not explicitly exhibited the additional contributions to the $F_{1,5}^{n,c}$ form factors that arise from the gaugino admixtures of the neutralinos and charginos. These are proportional to the electroweak gauge couplings and are therefore not enhanced by a large top-quark Yukawa coupling. These contributions have been neglected in our present analysis. We have also not exhibited the electroweak-like corrections to the incoming part of the diagram, that involve loops of first-generation squarks and neutralinos or charginos. These corrections are rather small as the relation $m_q \approx m_{\tilde{q}} + m_\chi$, that the numerical analysis below shows is required for enhancement, is not satisfied in this case.

The QCD-like corrections involve self-energy, vertex, and box diagrams. In the approximation of neglecting the box diagrams,² one can readily obtain the shifts in the total parton-level cross sections and cast them in the same format as the electroweak-like corrections given above. In this form comparison between the two classes of corrections becomes transparent. The QCD-like one-loop correction becomes

$$\Delta\hat{\sigma}^{\text{QCD}} = \frac{8\pi\alpha_s^2}{9\hat{s}^2} \beta_t \left(\frac{\alpha_s}{4\pi} \right) \left[\frac{2}{3}(\hat{s} + 2m_t^2)(F_1^t + F_1^q) + 2F_5^t m_t \hat{s} \right]. \quad (11)$$

The form factor F_1^t , which modifies the outgoing part of the diagram is given by

$$\begin{aligned} F_1^t = & \sum_{J=1}^2 \left\{ \left(-\frac{1}{3}\right)[c_{24} + m_t^2(c_{11} + c_{21})]^{(\tilde{g}\tilde{t}_J\tilde{t}_J)} + \left(\frac{4}{3}\right)[F_1^{t\tilde{g}\tilde{t}_J} + 2m_t^2 G_1^{t\tilde{g}\tilde{t}_J}] \right. \\ & + (-1)^J \sin(2\theta_t) m_t m_{\tilde{g}} \left[\left(\frac{1}{3}\right)(c_0 + c_{11})^{(\tilde{g}\tilde{t}_J\tilde{t}_J)} + \left(\frac{8}{3}\right)G_0^{t\tilde{g}\tilde{t}_J} \right] \\ & + \left(\frac{3}{2}\right)\left[-\frac{1}{2} + 2c_{24} + \hat{s}(c_{22} - c_{23}) - m_{\tilde{g}}^2 c_0 - m_t^2(c_0 + 2c_{11} + c_{21}) \right. \\ & \left. \left. - (-1)^J 2\sin(2\theta_t) m_t m_{\tilde{g}}(c_0 + c_{11}) \right]^{(\tilde{t}_J\tilde{g}\tilde{g})} \right\}, \quad (12) \end{aligned}$$

where θ_t is the top-squark mixing angle, and the superscripts (*abb*) indicate that the corresponding c functions depend on $(-p_3, p_3 + p_4, m_a, m_b, m_b)$. One also defines [8]

$$F_1^{t\tilde{q}\tilde{t}_J} = \int_0^1 dy y \ln \left[\frac{-m_t^2 y(1-y) + m_{\tilde{g}}^2(1-y) + m_{\tilde{t}_J}^2 y}{\mu^2} \right], \quad (13)$$

$$G_n^{t\tilde{q}\tilde{t}_J} = - \int_0^1 dy \frac{y^{n+1}(1-y)}{-m_t^2 y(1-y) + m_{\tilde{g}}^2(1-y) + m_{\tilde{t}_J}^2 y}. \quad (14)$$

In the expression for $F_1^{t\tilde{q}\tilde{t}_J}$, μ^2 is the renormalization-group scale that appears in the dimensional regularization procedure. One can verify that the full one-loop correction is independent of the choice of μ^2 , as expected.

The analogous form factor that modifies the incoming part of the diagram (F_1^q) is obtained from F_1^t by setting $\tilde{t}_J \rightarrow \tilde{q}_J$, $m_t \rightarrow m_q$, $\theta_t \rightarrow \theta_q$, and by replacing p_3, p_4 by p_1, p_2 , the incoming quark and anti-quark momenta. Since $m_q \approx 0$, the expression

²Recent calculations of supersymmetric QCD corrections to light-quark scattering at the Tevatron indicate that box diagram contributions are indeed small near the threshold region [19].

for F_1^q simplifies considerably. Note the close resemblance between the first two lines in F_1^t and the expression for F_1^n in Eq. (7) above, as both form factors originate from analogous diagrams ($\chi_j^0 \leftrightarrow \tilde{g}$); the differences in the coefficients stem from of the color factors that appear in the QCD-like diagram. In contrast, the last two lines in F_1^t correspond to a new diagram (not present in the electroweak-like case) where the gluino couples directly to the gluon and which carries a large color factor. We also have

$$F_5^t = \sum_{J=1}^2 \left\{ \left(\frac{1}{6} \right) [m_t(c_{11} + c_{21}) - (-1)^J \sin(2\theta_t) m_{\tilde{g}}(c_0 + c_{11})]^{(\tilde{g}\tilde{t}_J\tilde{t}_J)} + \left(\frac{3}{2} \right) [m_t(c_{11} + c_{21}) + (-1)^J \sin(2\theta_t) m_{\tilde{g}} c_{11}]^{(\tilde{t}_J\tilde{g}\tilde{g})} \right\}, \quad (15)$$

where we again note the resemblance (up to the color factor coefficient) between the first term in F_5^t and its counterpart F_5^n in Eq. (8). The second term in F_5 corresponds to the diagram not present in the electroweak-like case. The analogous form factor F_5^q (that arises from the incoming part of the diagram) is obtained from F_5^t by setting $\tilde{t}_J \rightarrow \tilde{q}_J$, $m_t \rightarrow m_q$, $\theta_t \rightarrow \theta_q$, by introducing an overall minus sign, and by replacing p_3, p_4 by p_1, p_2 , the incoming quark and anti-quark momenta. This contribution is negligible since $m_q \approx 0$ and because in the MSSM $\theta_q \propto m_q \approx 0$. Our results for the supersymmetric QCD corrections agree with those presented earlier in Ref. [8], and its erratum [20].

The actual observable cross section is obtained by integrating $\hat{\sigma} + \Delta\hat{\sigma}$ over the parton distribution functions, *i.e.*,

$$\begin{aligned} \sigma + \Delta\sigma = & \int_{\tau_0}^1 d\tau \int_{\tau}^1 \frac{dx_1}{x_1} \left[u(x_1)u(x_2) + u(x_1)sea(x_2) + sea(x_1)u(x_2) \right. \\ & + d(x_1)d(x_2) + d(x_1)sea(x_2) + sea(x_1)d(x_2) \\ & \left. + 6sea(x_1)sea(x_2) \right] (\hat{\sigma} + \Delta\hat{\sigma})(\hat{s}), \end{aligned} \quad (16)$$

where $\tau_0 = 4m_t^2/s$, $x_2 = \tau/x_1$, $\hat{s} = \tau s$, and the parton distribution functions (u, d, sea) are taken from Ref. [21] setting the scale $Q = m_t$.

3 Numerical results

Inspecting the above formulas, one can immediately get an idea of the typical size of the one-loop corrections, as they are proportional to

$$\frac{\Delta\hat{\sigma}^{\text{EW}}}{\hat{\sigma}} \propto \left(\frac{\lambda_t}{4\pi} \right)^2, \quad \frac{\Delta\hat{\sigma}^{\text{QCD}}}{\hat{\sigma}} \propto \left(\frac{\alpha_s}{4\pi} \right). \quad (17)$$

For the favored values of m_t , both these factors are $\sim 1\%$. We thus see that unless there are dynamical enhancements within the loop factors contributing to these diagrams, both contributions are comparable in size, and more importantly, much too

small to be disentangled from the Standard Model contribution, or to be observed experimentally at the Tevatron or any of its planned or proposed upgrades.

Such dynamical enhancements are however possible for restricted ranges of the mass parameters. The top-quark self-energy diagrams show one such enhancement through the B'_0, B'_1 functions when $m_t \approx m_a + m_b$, where $m_{a,b}$ are the masses of the two particles entering the two-point function. The enhancement occurs right below the threshold for $t \rightarrow a + b$ decay. For the top quark there are three possibilities for $m_{a,b}$: $(m_{\tilde{t}_{1,2}}, m_{\chi_{1,2,3,4}^0})$; $(m_{\tilde{b}_{1,2}}, m_{\chi_{1,2}^\pm})$; and $(m_{\tilde{t}_{1,2}}, m_{\tilde{g}})$. Given the present experimental lower limits on the squark (excluding \tilde{t}) and gluino masses (*i.e.*, $m_{\tilde{g}}, m_{\tilde{g}} > 175$ GeV; $m_{\tilde{g}} \approx m_{\tilde{g}} > 230$ GeV [22]), only the first possibility may be realized. That is, enhancements may occur for $m_t \approx m_{\tilde{t}_{1,2}} + m_{\chi_{1,2,3,4}^0}$. Moreover, these enhancements will be maximized when the neutralinos have a high higgsino content. (We do not see such enhancements for the incoming part of the diagram because $m_q \approx 0$.)

In this region of parameter space (and for real values of N_{j4}) one obtains the following approximate expression

$$\begin{aligned} \frac{\Delta\hat{\sigma}}{\hat{\sigma}} &\approx \left(\frac{\lambda_t}{4\pi}\right)^2 \sum_{j=1}^4 (N_{j4})^2 \sum_{J=1}^2 2 \left[m_t^2 B'_1 - (-1)^{J+1} \sin(2\theta_t) m_t m_{\chi_j^0} B'_0 \right] \\ &\rightarrow \left(\frac{\lambda_t}{4\pi}\right)^2 \sum_{J=1}^2 2 \left[m_t^2 B'_1 - (-1)^{J+1} \sin(2\theta_t) m_t m_\chi B'_0 \right], \end{aligned} \quad (18)$$

where the second expression follows when one of the neutralinos (χ) carries the full higgsino admixture. Also, the choice $\tan\beta = 1$ maximizes λ_t for a fixed value of m_t . In this ‘best case scenario’, one can plot $\Delta\sigma/\sigma$ (*i.e.*, after integration over parton distribution functions) versus the neutralino mass (m_χ), and study the dependence on the top-squark masses and mixing angle. Note that the mixing-angle term does not contribute if the top-squark masses are degenerate.

In the case of degenerate masses, taken at $m_{\tilde{t}_1} = m_{\tilde{t}_2} = 50$ (75) GeV, the resulting relative shift (%), as a function of m_χ , is shown by the dotted curve on the upper-left-hand panel in Fig. 1(2).³ The large dips at $m_\chi \approx m_t - m_{\tilde{t}_{1,2}} \approx 125$ (100) GeV derive from the B'_1 term in Eq. (18) and have been regularized by setting $m_t^2 \rightarrow m_t^2 - im_t \Gamma_t$, where Γ_t (a few GeV) is the top-quark decay width.⁴ The depth of the dips depends on the value of m_χ/m_t at which it occurs, and is maximized for $m_\chi/m_t \approx 0.73$, which in this case implies $m_\chi \approx 128$ GeV, $m_{\tilde{t}} \approx 47$ GeV (*i.e.*, as in Fig. 1).

In a more realistic scenario, light top-squarks cannot be degenerate in mass because limits on additional contributions to the ρ parameter restrict the splitting between the \tilde{t}_L and $\tilde{b}_L \approx \tilde{b}_1$, and from direct experimental searches one estimates that $m_{\tilde{b}_1} > 200$ GeV. In the case of no top-squark mixing ($\theta_t = 0, \pi/2$), the splitting of $\tilde{t}_{1,2}$

³The numerical results in the figures have been obtained for the ‘best case scenario’ of Eq. (18), but without neglecting the vertex corrections contained in the c functions.

⁴Throughout our numerical calculations we have used $m_t = 175$ GeV, $m_t \Gamma_t = 289$ GeV², and $\alpha_s = 0.118$.

leads to a double-dip structure if both top-squark masses are such that $m_t \approx m_{\tilde{t}_{1,2}} + m_\chi$ can be satisfied, as in Fig. 1 (solid curve, upper-left-hand panel), where we have taken $m_{\tilde{t}_1} = 50$ GeV and $m_{\tilde{t}_2} = 100$ GeV. Note that the dips do not have the same depth, as discussed above. In Fig. 2 there is a single dip because we have taken $m_{\tilde{t}_1} = 75$ GeV and $m_{\tilde{t}_2} = 250$ GeV.

Yet more realistic is the case of top-squark mixing, which is naturally present in supergravity theories. This mixing tends to “screen” the contributions of top-squarks to the Z -pole observables [23], and therefore allows a larger $\tilde{t}_L - \tilde{b}_L$ mass splitting. In Figs. 1 and 2 we present the results for four choices of the mixing angle $\theta_t = 0, 0.10, 0.25$, and maximal mixing ($\frac{\pi}{4}$). The plots also apply for $\theta_t \rightarrow \frac{\pi}{2} - \theta_t$, which leaves $\sin(2\theta_t)$ unchanged. In this case the B'_0 function in Eq. (18) plays an important role, as it exhibits a similar dip behavior as B'_1 does, although with a different sign at each dip. This effect makes one dip deeper (corresponding to \tilde{t}_1) whereas the other one shallower (corresponding to \tilde{t}_2), as evidenced in Fig. 1. The effect can be very significant, completely eliminating one of the dips at maximum mixing angle. In Fig. 2 only the dip that gets deeper exists.

As explained above, the QCD corrections are not expected to exhibit the dip structure that the electroweak corrections possess, because the relation $m_t \approx m_{\tilde{g}} + m_{\tilde{t}}$ cannot be satisfied by the experimentally allowed gluino masses. In Fig. 3 we show the QCD correction versus the universal squark masses ($m_{\tilde{t}_{1,2}} = m_{\tilde{q}}$) for fixed values of the gluino mass. The curve for $m_{\tilde{g}} = 150$ GeV behaves differently from the others because for sufficiently light squark masses, the relation $m_t \approx m_{\tilde{g}} + m_{\tilde{q}}$ will be satisfied, *i.e.*, a dip occurs. This region of parameter space is disfavored experimentally; it is shown here to make contact with Ref. [20], with which we agree qualitatively. From Fig. 3 we see that shifts as large as $\sim 20\%$ may occur. We also observe that the corrections go to zero when the supersymmetric particle masses get large, *i.e.*, the expected decoupling effect. This figure also contains a curve (the dashed line) where all sparticle masses are taken to be the same ($m_{\tilde{g}} = m_{\tilde{t}_{1,2}} = m_{\tilde{q}}$), which is seen to intercept the other curves at the appropriate places, and to decouple rather quickly.

In order to explore the effects of lighter top-squark masses, we concentrate on the $m_{\tilde{q}} = m_{\tilde{g}}$ case⁵ (the dashed line in Fig. 3) and in Fig. 4 we plot the QCD corrections for representative choices of $(m_{\tilde{t}_1}, m_{\tilde{t}_2})$. For reference, the all-equal-masses case is shown as a dashed line (as in Fig. 3). We can see that light top-squark masses enhance the corrections, especially in the region $m_{\tilde{q}} = m_{\tilde{g}} \approx (200 - 250)$ GeV. This enhancement occurs (although to a lesser extent) even if only one of the top-squarks is light. We have also explored the effect of top-squark mixing, which is non-vanishing only if $m_{\tilde{t}_1} \neq m_{\tilde{t}_2}$. We find this effect to be rather small in the case of the QCD-like corrections amounting, for example, to a decrease in the peak value of the (50,250) curve in Fig. 4 by 15% for maximal mixing.

⁵The $m_{\tilde{q}} \approx m_{\tilde{g}}$ relation occurs naturally in supergravity theories.

4 Expectations in specific models

The results presented in the previous section should represent the largest one-loop supersymmetric shifts to be expected in the top-quark cross section. However, in specific regions of MSSM parameter space or specific supergravity models, the shifts are likely to be much smaller than the largest possible ones, as the conditions for enhancement may not be satisfied: large electroweak shifts require a higgsino-like neutralino, light top-squarks, $\tan \beta \approx 1$, and a specific relation between their masses (*i.e.*, $m_\chi + m_{\tilde{t}} \approx m_t$); large QCD shifts require $m_{\tilde{g}}, m_{\tilde{q}} < 250 \text{ GeV}$ and light top-squarks. Interestingly enough, various scenarios (*i.e.*, selected regions of MSSM parameter space) recently proposed to possibly explain some experimental measurements that appear to deviate from Standard Model expectations, fall *precisely* in the class of models that may lead to one-loop enhancements of the top-quark cross section.

The discrepancy between the LEP measured value of R_b and its prediction in the Standard Model may be alleviated by supersymmetric loop corrections to the $Zb\bar{b}$ vertex that involve charginos and top-squarks [9]. Moreover, $\tan \beta$ should be close to 1, the charginos should be higgsino-like (and correspondingly the neutralinos too), and the top-squarks should be right-handed. Both should be as light as LEP 1.5 searches allow [24]. Since in this scenario there are no restrictions on the squark or gluino masses, let us concentrate on the electroweak corrections, that will be significantly enhanced (negatively) in this case if the relation $m_\chi + m_{\tilde{t}} \approx m_t$ happens to be satisfied. This may indeed occur for $m_{\tilde{t}_2}$ (but not for the desired values of $m_{\tilde{t}_1}$ and m_χ , both below M_W).

In analogy with the so-called light-gluino window, it has been remarked that there is a light-higgsino window [10], where the Higgsino mixing parameter and the SU(2) gaugino mass are very small ($\mu, M_2 \approx 0$) and $\tan \beta \approx 1$. In this scenario there are three neutralinos with significant higgsino admixtures, two with masses close to M_Z and a very light one. Moreover, a light top-squark is also desired to enhance R_b^{susy} . Therefore, if $m_t \approx m_\chi + m_{\tilde{t}} \approx M_Z + m_{\tilde{t}}$ or equivalently $m_{\tilde{t}} \approx m_t - M_Z \approx 85 \text{ GeV}$, then the top-quark cross section will be shifted to lower values by a significant amount.

The last scenario we address has been advanced in Refs. [11, 12] as a possible explanation for the one much-publicized event at CDF, consisting of $ee\gamma\gamma$ plus missing energy. This event has been ascribed to selectron pair-production, with decay into electron and second-to-lightest neutralino (χ_2^0), and further radiative decay of the neutralino into the LSP ($\chi_2^0 \rightarrow \chi_1^0 + \gamma$). The missing energy is carried away by the pair of lightest neutralinos produced. The dominance of the (one-loop) radiative decay $\chi_2^0 \rightarrow \chi_1^0 + \gamma$ over the more traditional ones ($\chi_2^0 \rightarrow \chi_1^0 f \bar{f}$) provides the most important constraint on the parameter space, requiring a higgsino-like χ_1^0 and a photino-like χ_2^0 . This is achieved by setting the SU(2) and U(1) gaugino masses equal at the electroweak scale ($M_1 = M_2$ and $\tan \beta \approx 1$), precluding the gaugino mass unification in GUTs. Furthermore, the kinematics of the event appear to require: $m_{\chi_1^0} \approx (30 - 55) \text{ GeV}$ and $m_{\chi_2^0} \approx m_{\chi_1^0} + 30 \text{ GeV}$. To make contact with the supersymmetric enhancement of R_b , it is also assumed that the top-squark is light ($m_{\tilde{t}_1} \approx (45 - 60) \text{ GeV}$). In this case, however, the top-quark would have enhanced

decays to $\tilde{t} + \chi_1^0$, thus diluting the observed top-quark sample. To undo this effect, it has been further proposed [12] that squarks and gluinos should be as light as experimentally allowed ($m_{\tilde{g}} \approx (210 - 235)$ GeV, $m_{\tilde{q}} \approx (220 - 250)$ GeV) such that $\tilde{g} \rightarrow t\tilde{t}$ decays add to the top-quark sample significantly. (This mechanism was originally proposed in Ref. [25].) Given these values of the squark and gluino masses, from Fig. 4 one can see that we generally expect $\approx +15\%$ supersymmetric QCD corrections to the top-quark cross section. (There may also be significant electroweak corrections if $m_{\tilde{t}_2} \approx m_t - m_{\chi_1^0} \approx (105 - 145)$ GeV.)

Going beyond the specific models discussed above, the light top-squarks that enhance both electroweak and QCD corrections will likely decrease the canonical top-quark branching ratio into bW because of the availability of the supersymmetric decay channels $t \rightarrow \tilde{t} + \chi$. Indeed, the top-quark Yukawa coupling in Eq. (5) entails an enhanced coupling between the top-quark, a higgsino-like neutralino, and a right-handed top-squark. This situation is favored by the enhanced corrections discussed above, and therefore enhance the exotic decays of the top quark. At present there are no real experimental limits on $B(t \rightarrow bW)$, only on $B(t \rightarrow bW)/B(t \rightarrow qW)$ [26]. The only limits on $B(t \rightarrow bW)$ have been obtained by correlating the top-quark mass and cross section measurements with the Standard Model cross section, implying $B(t \rightarrow \text{other}) < 25\%$ [27]. If the electroweak (negative) correction occurs when the exotic channel ($t \rightarrow \tilde{t}\chi$) is kinematically allowed, the yield of $bWbW$ events will be decreased by the two effects, implying an effective $B(t \rightarrow bW)$ ratio as small as $(0.65)(0.5) \approx 0.3$, assuming a -35% shift in the cross section and $B(t \rightarrow \tilde{t}\chi) = 1/2$. However, we note that the enhancements to the electroweak corrections occur right *below* the threshold for top-quark decay into top-squark and neutralino (see Figs. 1,2), and therefore the exotic decay channel is effectively closed.

Recent complementary studies of top-quark properties in supersymmetric theories include supersymmetric one-loop corrections to the $t \rightarrow \tilde{t}\chi$ exotic decay channel [28], supersymmetric three-body decays of the top quark [29], and one-loop supersymmetric corrections to the top-quark width [30].

5 Conclusions

The experimental study of the top quark has just begun in earnest, with its mass and cross section having been measured to some precision. The Main Injector upgrade of the Tevatron should essentially provide a top-quark factory, where observations will be confronted with theoretical expectations for cross sections and branching ratios. We have shown that these precise measurements may indeed point to deviations from the Standard Model, as may be expected in supersymmetric theories. These deviations may be quite sizeable and therefore easy to detect, especially in scenarios with rather light sparticles that have been proposed to explain various apparent experimental anomalies. In the longer term, the presence of top quarks at the LHC will constitute one of largest backgrounds in new physics searches. Therefore, it will be essential to have a very good understanding of top-quark physics beforehand, so that these

backgrounds may be subtracted off appropriately.

Acknowledgments

We would like to thank Jin Min Yang for useful discussions. R.R. would also like to thank Toby Falk and David Robertson for useful discussions. The work of J.K. and R.R. has been supported by the World Laboratory. The work of J. L. has been supported in part by DOE grant DE-FG05-93-ER-40717. The work of D.V.N. has been supported in part by DOE grant DE-FG05-91-ER-40633.

References

- [1] CDF Collaboration, F. Abe et al., Phys. Rev. Lett. **74** (1995) 2676; D0 Collaboration, S. Abachi et al., Phys. Rev. Lett. **74** (1995) 2632.
- [2] A. Caner (CDF Collaboration), presented at the 1996 La Thuile Conference; M. Narain (D0 Collaboration), presented at the 1996 La Thuile Conference.
- [3] “Future ElectroWeak Physics at the Fermilab Tevatron”, Report of the TeV 2000 Working Group, FERMILAB-PUB-96/046, edited by D. Amidei and R. Brock.
- [4] E. Laenen, J. Smith, and W. van Neerven, Nucl. Phys. B **369** (1992) 543 and Phys. Lett. B **321** (1994) 254.
- [5] E. Berger and H. Contopanagos, Phys. Lett. B **361** (1995) 115 and hep-ph/9603326.
- [6] S. Catani, M. Mangano, P. Nason, and L. Trentadue, hep-ph/9602208.
- [7] J. Yang and C. Li, Phys. Rev. D **52** (1995) 1541.
- [8] C. Li, B. Hu, J. Yang, and C. Hu, Phys. Rev. D **52** (1995) 5014.
- [9] J. D. Wells, C. Kolda, and G. L. Kane, Phys. Lett. B **338** (1994) 219; D. Garcia, R. Jimenez, and J. Sola, Phys. Lett. B **347** (1995) 321; D. Garcia and J. Sola, Phys. Lett. B **357** (1995) 349; X. Wang, J. L. Lopez, and D. V. Nanopoulos, Phys. Rev. D **52** (1995) 4116; J. Wells and G. Kane, Phys. Rev. Lett. **76** (1996) 869; J. Ellis, J. L. Lopez, and, D. V. Nanopoulos, Phys. Lett. B **372** (1996) 95; A. Brignole, F. Feruglio, and F. Zwirner, hep-ph/9601293; P. Bamert, *et. al.*, hep-ph/9602438; P. Chankowski and S. Pokorski, hep-ph/9603310.
- [10] J. Feng, N. Polonsky, and S. Thomas, Phys. Lett. B **370** (1996) 95.
- [11] S. Ambrosanio, G. Kane, G. Kribs, S. Martin, and S. Mrenna, Phys. Rev. Lett. **76** (1996) 3498; S. Dimopoulos, M. Dine, S. Raby, and S. Thomas, Phys. Rev. Lett. **76** (1996) 3502; G. Kane and J. Wells, hep-ph/9603336.

- [12] G. Kane and S. Mrenna, hep-ph/9605351.
- [13] S. Park (CDF Collaboration), in Proceedings of the 10th Topical Workshop on Proton-Antiproton Collider Physics, Fermilab (May 1995).
- [14] H. Haber and G. Kane, Phys. Rep. **117** (1985) 75; J. Gunion and H. Haber, Nucl. Phys. B **272** (1986) 1.
- [15] G. Passarino and M. Veltman, Nucl. Phys. B **160** (1979) 151.
- [16] G.J. van Oldenborgh and J.A.M. Vermaseren, Z. Phys. C **46** (1990) 425.
- [17] J. Yang and C. Li, erratum to Ref. [7] (to appear).
- [18] J. Yang and C. Li, hep-ph/9603442.
- [19] P. Kraus and F. Wiczek, hep-ph/9601279; J. Ellis and D. Ross, hep-ph/9604432.
- [20] C. Li, B. Hu, J. Yang, and C. Hu, Phys. Rev. D **53** (1996) 4112.
- [21] J. Morfin and W. Tung, Z. Phys. C **52** (1991) 13.
- [22] S. Abachi, *et. al.* (D0 Collaboration), Phys. Rev. Lett. **75** (1995) 618; F. Abe, *et. al.* (CDF Collaboration), Phys. Rev. Lett. **69** (1992) 3439 and Phys. Rev. Lett. **76** (1996) 2006; J. Hauser, in Proceedings of the 10th Topical Workshop on Proton-Antiproton Collider Physics, Fermilab, 1995, edited by R. Raja and J. Yoh (AIP, New York, 1995), p. 13.
- [23] A. Dabelstein, W. Hollik, and W. Mosle, hep-ph/9506251 and references therein.
- [24] D. Buskulic, *et. al.* (ALEPH Collaboration), Phys. Lett. B **373** (1996) 24; L. Dijkstra (DELPHI Collaboration), CERN-PPE-95-004; M. Acciarri, *et. al.* (L3 Collaboration), CERN-PPE-96-029; G. Alexander, *et. al.* (OPAL Collaboration), CERN-PPE-96-020.
- [25] T. Kon and T. Nonaka, Phys. Rev. D **50** (1994) 6005.
- [26] J. Incandela (CDF Collaboration), FERMILAB-CONF-95-237-E (July 1995); T. LeCompte (CDF Collaboration), FERMILAB-CONF-96/021-E (January 1996).
- [27] X. Wang, J. L. Lopez, and D. V. Nanopoulos, in Ref. [9]; S. Mrenna and C. P. Yuan, Phys. Lett. B **367** (1996) 188.
- [28] A. Djouadi, W. Hollik, and C. Junger, hep-ph/9605340.
- [29] J. Guasch and J. Sola, hep-ph/9603441.
- [30] J. Sola, hep-ph/9605306.

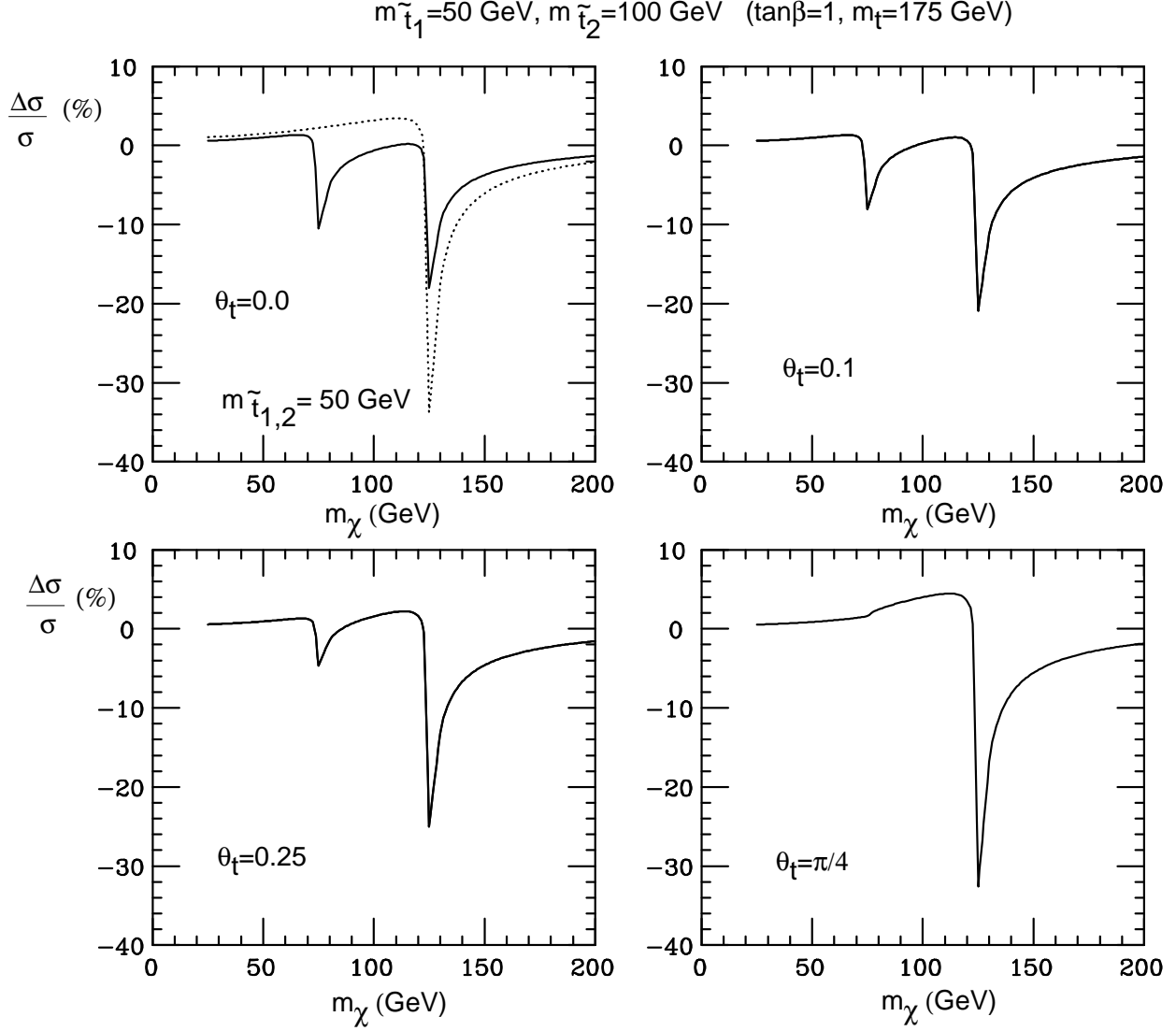


Figure 1: The relative (%) one-loop supersymmetric electroweak correction to the top-quark pair-production cross section at the Tevatron as a function of the (higgsino-like) neutralino mass, for $m_t = 175 \text{ GeV}$, $\tan\beta = 1$, $m_{\tilde{t}_1} = 50 \text{ GeV}$, $m_{\tilde{t}_2} = 100 \text{ GeV}$, and various choices of the top-squark mixing angle ($\theta_t = 0.0, 0.10, 0.25, \frac{\pi}{4}$). The dotted curve on the upper-left-hand panel corresponds to $m_{\tilde{t}_1} = m_{\tilde{t}_2} = 50 \text{ GeV}$. Note the dips on the curves when $m_t \approx m_{\tilde{t}_{1,2}} + m_\chi$.

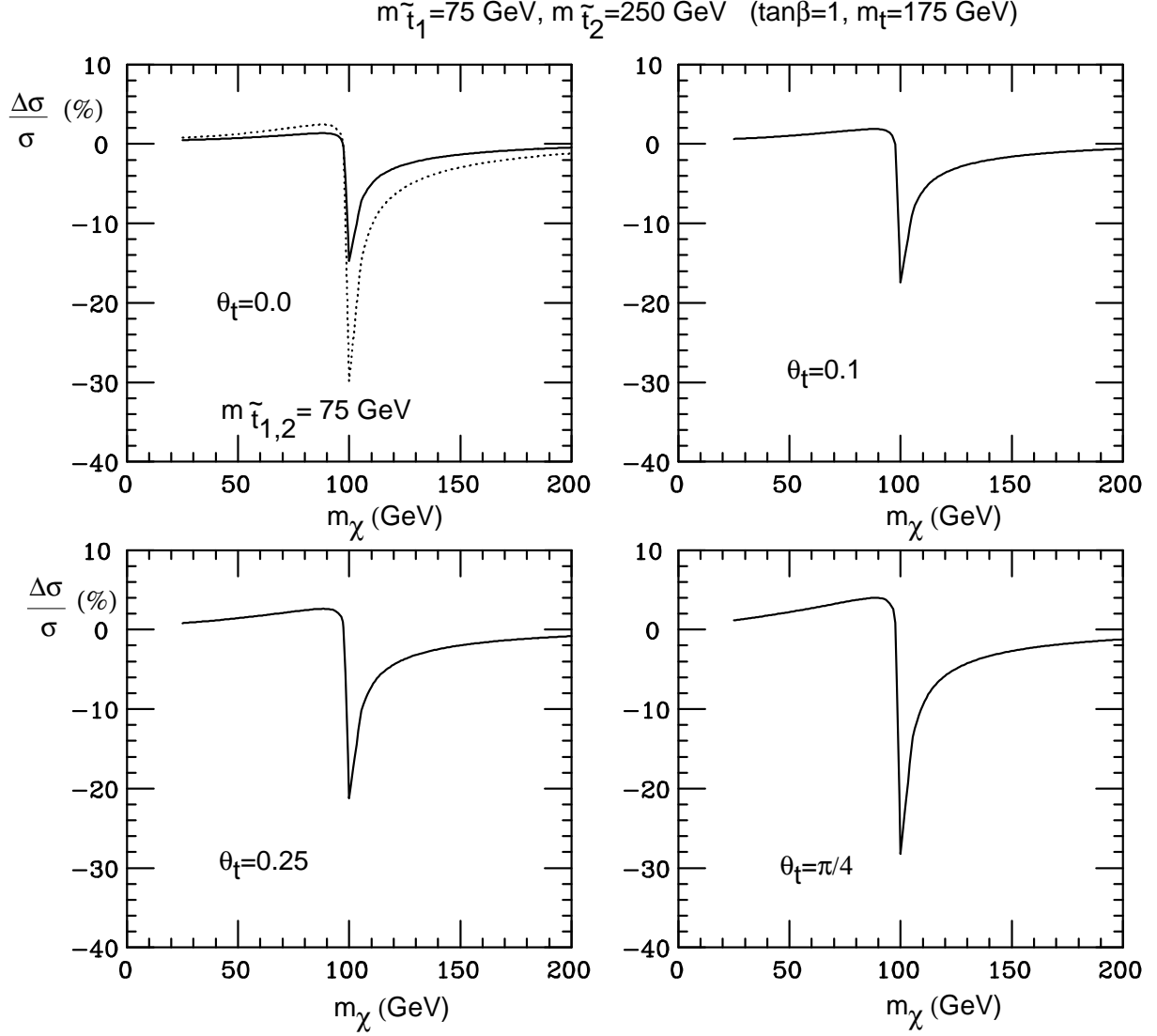


Figure 2: The relative (%) one-loop supersymmetric electroweak correction to the top-quark pair-production cross section at the Tevatron as a function of the (higgsino-like) neutralino mass, for $m_t = 175 \text{ GeV}$, $\tan\beta = 1$, $m_{\tilde{t}_1} = 75 \text{ GeV}$, $m_{\tilde{t}_2} = 250 \text{ GeV}$, and various choices of the top-squark mixing angle ($\theta_t = 0.0, 0.10, 0.25, \frac{\pi}{4}$). The dotted curve on the upper-left-hand panel corresponds to $m_{\tilde{t}_1} = m_{\tilde{t}_2} = 75 \text{ GeV}$. Note the dips on the curves when $m_t \approx m_{\tilde{t}_{1,2}} + m_\chi$.

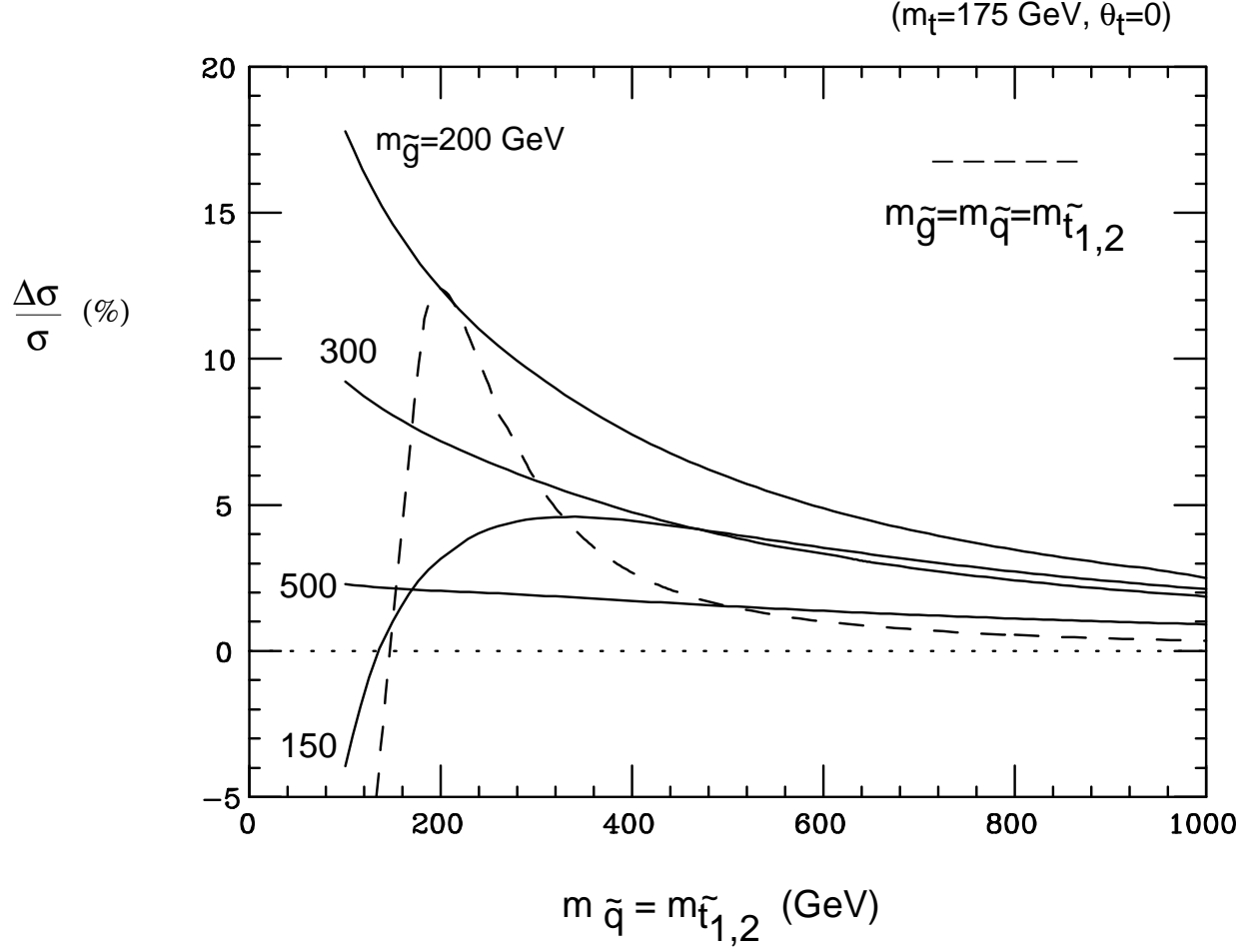


Figure 3: The relative (%) one-loop supersymmetric QCD correction to the top-quark pair-production cross section at the Tevatron as a function of the universal squark mass, for $m_t = 175$ GeV and the indicated choices of the gluino mass. The dashed curve represents the $m_{\tilde{g}} = m_{\tilde{q}}$ case.

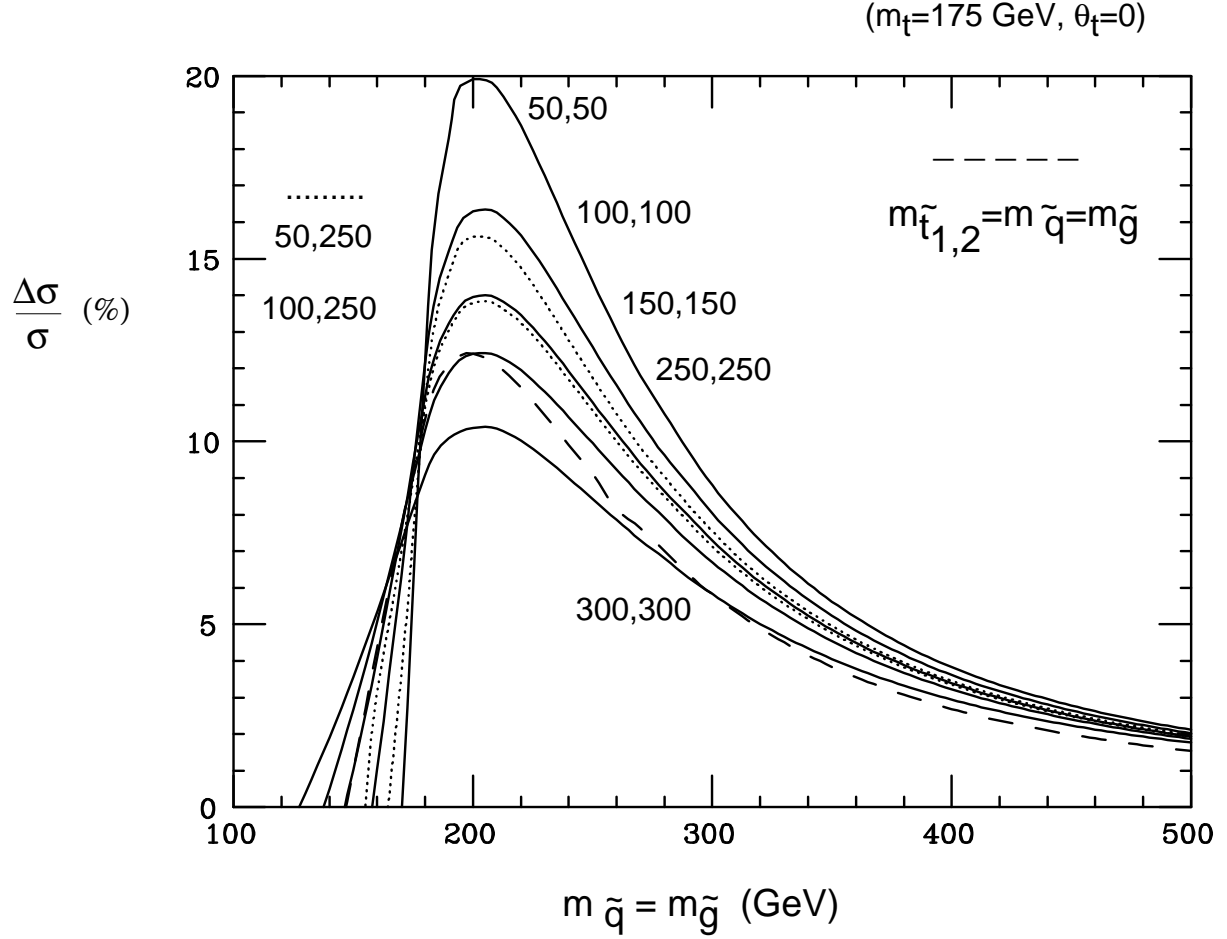


Figure 4: The relative (%) one-loop supersymmetric QCD correction to the top-quark pair-production cross section at the Tevatron as a function of the squark or gluino mass, for $m_t = 175$ GeV and for the indicated choices of top-squark masses ($m_{\tilde{t}_1}, m_{\tilde{t}_2}$). The dotted curves highlight the effect of non-degenerate top-squark masses. The dashed curve represents the fully degenerate $m_{\tilde{t}_{1,2}} = m_{\tilde{g}} = m_{\tilde{q}}$ case.